CORA Cork Open Research Archive
Cartlann Taighde Oscailte Chorcaí

UCC

University College Cork, Ireland
Coláiste na hOllscoile Corcaigh

Mechanism for zirconium oxide atomic layer deposition using bis(methylcyclopentadienyl)methoxymethyl zirconium

J. W. Elam and M. J. PellinS. D. Elliott and A. ZydorM. C. Faia and J. T. Hupp

Mechanism for zirconium oxide atomic layer deposition using bis(methylcyclopentadienyl)methoxymethyl zirconium

J. W. Elam[a)] and M. J. Pellin
Argonne National Laboratory, Argonne, Illinois 60439, USA

S. D. Elliott and A. Zydor
Tyndall National Institute, Lee Maltings, Cork, Ireland

M. C. Faia and J. T. Hupp
Department of Chemistry, Northwestern University, Evanston, Illinois 60208, USA

The mechanism for zirconium oxide atomic layer deposition using bis(methylcyclopentadienyl)methoxymethyl zirconium and H_2O was examined using *ab initio* calculations of hydrolysis energies to predict the order of ligand loss. These predictions were tested using *in situ* mass spectrometric measurements which revealed that the methyl ligand, and 65% of the methylcyclopentadienyl ligands are lost during the zirconium precursor adsorption. The remaining 35% of the methylcyclopentadienyl ligands and the methoxy ligand are lost during the subsequent H_2O exposure. These measurements agree very well with the predictions, demonstrating that thermodynamic calculations are a simple and accurate predictor for the reactivities of these compounds. © *2007 American Institute of Physics*. [DOI: 10.1063/1.2824814]

Atomic layer deposition (ALD) is a thin film growth method using alternating, self-limiting reactions between gaseous precursors and a solid surface to deposit materials in an atomic layer-by-layer fashion.[1] Zirconium oxide (ZrO_2) is a promising high-dielectric constant replacement for SiO_2 in future microelectronic devices,[2] and also has applications in photovoltaics[3] and catalysis.[4] ALD is an attractive method for preparing ZrO_2 thin films because it affords precise thickness control and superb conformality.[5] Understanding the ALD mechanism is important because the mechanism affects the growth rate and purity of the films. Additionally, a mechanistic understanding can guide proper precursor selection. In this study, *ab initio* calculations are performed to predict the order in which the ligands are lost during ZrO_2 ALD. These predictions are tested using *in situ* quadrupole mass spectrometry (QMS).

We focus on the heteroleptic precursor, bis(methyl-cyclopentadienyl)methoxymethyl zirconium $[Zr(MeCp)_2(Me)(OMe)]$, abbreviated as ZrL_4, with ligands $L=MeCp$, Me, and OMe. Heteroleptic precursors facilitate mechanistic studies and allow precursor fine tuning. The Zr and Hf versions of this precursor are thermally stable to 500 °C (Ref. 6) and produce high quality dielectric films.[7] Using H_2O as oxygen source, the expected ALD reaction is

$$ZrL_{4(gas)} + 2H_2O_{(gas)} \rightarrow ZrO_{2(solid)} + 4HL_{(gas)}. \quad (1)$$
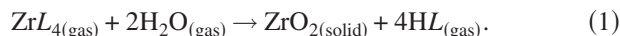
Equation (1) provides no information about the surface-mediated mechanism of growth or about the order of ligand release. This information is relevant because steric hindrance between the ligands remaining after the ZrL_4 pulse will dictate the ALD growth rate.[8]

At the start of the ZrL_4 pulse, the growing surface is covered with hydroxyls (surf-OH) that provide protons (H^+). The adsorption of ZrL_4 produces ligands on the surface ($L^-=MeCp^-$, Me^-, and OMe^-), which can combine with pro-

tons and desorb as HL. The kinetics of this elimination reaction will be determined by the relative bond strengths[9] of $Zr-L$ versus $H-L$ at the surface, and by surface properties such as the O–H strength and H^+ diffusion rate. To compare different ligands, it is adequate to compute the different $Zr-L$ versus $H-L$ bond enthalpies and to ignore effects that are specific to surface geometry.[10]
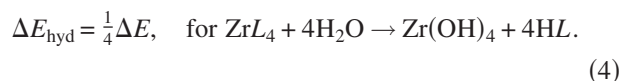
We define the gas-phase Brønsted basicity (BB) of L^- relative to OH^- as

$$\Delta E_{BB} = \Delta E, \quad \text{for } L^- + H_2O \rightarrow HL + OH^-. \quad (2)$$
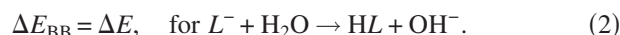
The more negative the ΔE_{BB}, the stronger the BB of L^- and the stronger the $H-L$ bond. We compute the change in internal energy neglecting entropy/temperature effects. We likewise define the Lewis basicity (LB) of L^- relative to OH^- as

$$\Delta E_{LB} = \tfrac{1}{4}\Delta E, \quad \text{for } 4L^- + Zr(OH)_4 \rightarrow ZrL_4 + 4OH^-. \quad (3)$$
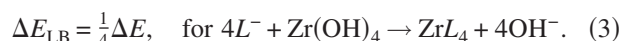
Stronger Lewis bases with strong $Zr-L$ bonding show more negative ΔE_{LB}. Combining these equations, $\Delta E_{hyd} = \Delta E_{BB} - \Delta E_{LB}$, where

$$\Delta E_{hyd} = \tfrac{1}{4}\Delta E, \quad \text{for } ZrL_4 + 4H_2O \rightarrow Zr(OH)_4 + 4HL. \quad (4)$$

Negative ΔE_{hyd} corresponds to an exoergic hydrolysis reaction at $T=0$ K. ΔE_{hyd} thus reflects the relative strengths of Zr^{4+} and H^+ bonding to L^-, using H_2O and $Zr(OH)_4$ as common reference molecules. Equation (4) is thus a *model* reaction for HL elimination whenever surf-OH and surf-L are present. The resemblance of Eq. (4) to the overall growth reaction with H_2O as precursor [Eq. (1)] is coincidental, since Eq. (1) contains no useful mechanistic information.

The species in Eq. (4) were modeled as isolated molecules in vacuum. The ground state electronic wavefunction of each molecule was calculated self-consistently within Kohn-Sham density functional theory (DFT) using TURBO-MOLE (Ref. 11) with the B-P86 functional,[12] an atom-centered SV(P) basis set,[18] and a 28-electron effective core

TABLE I. Computed energies (kJ/mol) for ligands in model ALD reactions. The Brønsted basicity ΔE_{BB} is from Eq. (2), the Lewis basicity ΔE_{LB} from Eq. (3), and the hydrolysis energy $\Delta E_{hyd} = \Delta E_{BB} - \Delta E_{LB}$ from Eq. (4). The ligand with the most negative ΔE_{hyd} is predicted to be eliminated first.

Ligand	Elimination product	ΔE_{BB}	ΔE_{LB}	ΔE_{hyd}
Me	CH_4	−46.9	+176.6	−223.5
MeCp	MeCpH	+274.7	+375.1	−100.4
OMe	MeOH	+160.9	+152.5	+8.4

potential on Zr.[13] All species were closed shell. Unconstrained optimization of the molecular geometry was carried out on the DFT potential energy hypersurface, but a vibrational analysis was not carried out. This method has been applied previously to heteroleptic Zr precursors.[14]

The calculated energetics are shown in Table I. The computed BB values decrease as MeCp > OMe > Me. The computed LB values are similar for Me and OMe but larger for MeCp. Applying Eq. (4), ΔE_{hyd} increases as OMe > MeCp > Me. We therefore predict that Me ligands will be eliminated first during the ZrL_4 pulse, followed by MeCp ligands if there are sufficient surf-OH. The OMe ligands along with some MeCp should be eliminated during the H_2O pulse.

To test these predictions, ZrO_2 ALD was monitored by QMS (Ref. [15]) (Stanford Research Systems RGA300) in a viscous flow reactor[16] at 350 °C using alternating exposures to $Zr(MeCp)_2(Me)(OMe)$ (Epichem) for 3 s and de-ionized H_2O for 1 s with 5 s purge periods between exposures. The $Zr(MeCp)_2(Me)(OMe)$ was vaporized at 95 °C. We verified that these conditions yield self-limiting ZrO_2 ALD using ellipsometric analysis of films deposited on silicon. The QMS signals arise from reactions occuring on the hot walls of the reactor, and no substrate is installed during these measurements.

The top three solid traces in Fig. 1 present the $m/z=79$, $m/z=16$, and $m/z=31$ QMS signals recorded during ZrO_2 ALD. The dotted lines at the bottom of the figure show the dosing times for the $Zr(MeCp)_2(Me)(OMe)$ and H_2O precursors with a high value designating an exposure to the indicated precursor. The middle portion of the graph between 30 and 92 s shows $4\frac{1}{2}$ ALD cycles in which the $Zr(MeCp)_2(Me)(OMe)$ and H_2O precursors are pulsed sequentially. Between 0 and 30 s, only the $Zr(MeCp)_2(Me)(OMe)$ precursor is pulsed to measure the background for this compound. Similarly, only the H_2O is pulsed between 92 and 120 s to evaluate the H_2O background. Note that during the background measurements, both a 1 s exposure followed by a 5 s exposure are used to maintain the same timing sequence as in the ALD cycles.

During the ZrO_2 ALD cycles, $m/z=31$ peaks are only observed during the H_2O exposures and the corresponding background is small (~15%), indicating that the methoxy ligand (–OMe) is released exclusively during the H_2O reaction. Similar results were obtained monitoring $m/z=32$ in agreement with the cracking pattern for methanol[17] produced by the reaction of methoxy ligands with the hydroxylated surface.

The $m/z=16$ trace in Fig. 1 shows the amount of CH_4 released during the ZrO_2 ALD along with the corresponding background measurements performed as described above. Peaks in the $m/z=16$ signal are observed when dosing both the $Zr(MeCp)_2(Me)(OMe)$ and H_2O precursors. However,
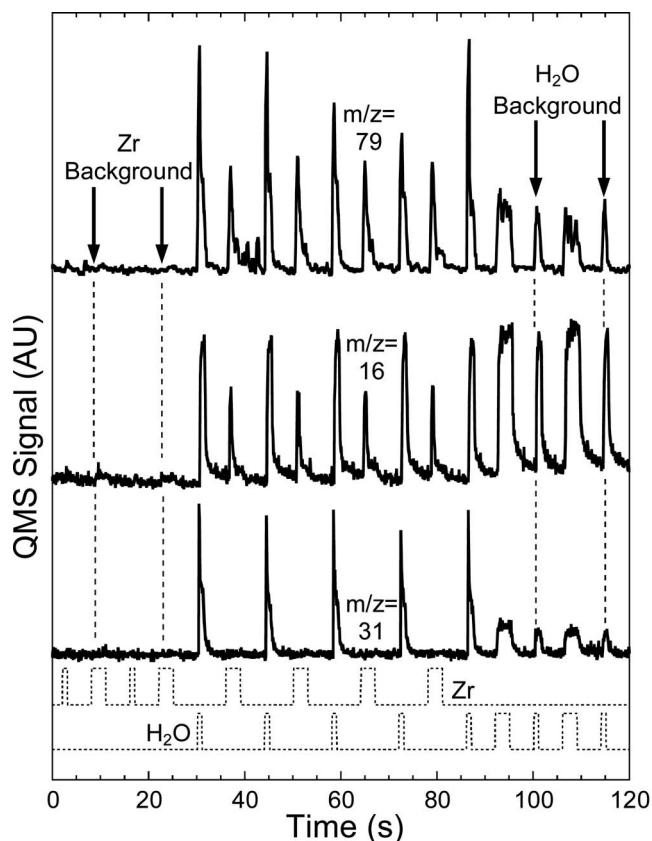

FIG. 1. QMS signals for $m/z=31$ (MeOH), $m/z=16$ (CH_4), and $m/z=79$ (MeCpH) measured during ZrO_2 ALD. The $Zr(MeCp)_2(Me)(OMe)$ and H_2O doses are indicated by the dotted lines at the bottom. The $Zr(MeCp)_2(Me)(OMe)$ and H_2O background signals are measured before and after the $4\frac{1}{2}$, consecutive ZrO_2 ALD cycles as indicated.

while the $Zr(MeCp)_2(Me)(OMe)$ background is negligible at $m/z=16$, the H_2O background and ALD signals are identical within the experimental error. Consequently, CH_4 is only released during the $Zr(MeCp)_2(Me)(OMe)$ exposures of the ZrO_2 ALD.

The $m/z=79$ signals attributed to methylcyclopentadiene (MeCpH) formed during the ZrO_2 ALD in Fig. 1 reveal that MeCpH is released during both of the precursor exposures. Similar results were obtained using $m/z=80$, and 77 consistent with the cracking pattern for HCpMe.[17] Integration of the $m/z=79$ peaks shows that, while the $Zr(MeCp)_2(Me)(OMe)$ background is negligible, 44% of the signal observed during the H_2O exposures is background. After background correction, we conclude that 65(±10)% of the CpMe ligands are eliminated during the $Zr(MeCp)_2(Me)(OMe)$ exposures, and the remaining 35(±14)% are released during the subsequent H_2O exposures.
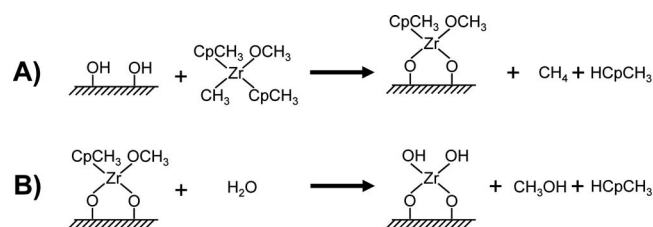

FIG. 2. Illustration of proposed ZrO_2 ALD mechanism.

The calculations and measurements suggest the mechanism for ZrO_2 ALD in Fig. 2. In step A, $Zr(MeCp)_2(Me)(OMe)$ reacts with the hydroxylated surface releasing the Me ligand as CH_4 and one or more of the MeCp ligands as MeCpH. This modified surface is exposed to H_2O in step B, liberating any remaining MeCp ligands as MeCpH, and all of the OMe ligands as MeOH. The QMS measurements indicate that, on average, 1.3 MeCp ligands are removed in step A, so that 30% of the $Zr(MeCp)_2(Me)(OMe)$ molecules react with three hydroxyls and release both MeCp ligands in step A.

Following the $Zr(MeCp)_2(Me)(OMe)$ adsorption, the surface is covered with MeCp and OMe in the ratio $\sim 2:3$. Consequently, the steric bulk of these ligands will limit the ALD growth rate. However, because the Me ligand is eliminated before saturation, replacing the Me with a bulkier alkyl group should not affect the growth rate.

The QMS measurements follow the ligand release pattern suggested by the ΔE_{hyd} calculations in Table I. This agreement supports our assertion that a simple comparison of bond strengths captures the essential information for predicting the ALD mechanism. Furthermore, we have identified the important precursor properties: strong affinity of Me for H^+ of surf-OH, weak bonding of MeCp to Zr, and similar bonding of OMe to Zr and H.

[1] M. Ritala and M. Leskelä, in *Handbook of Thin Film Materials*, edited by H. S. Nalwa (Academic, San Diego, 2001), Vol. 1, p. 103.

[2] G. D. Wilk, R. M. Wallace, and J. M. Anthony, J. Appl. Phys. **89**, 5243 (2001).

[3] D. B. Menzies, Q. Dai, L. Bourgeois, R. A. Caruso, Y. B. Cheng, G. P. Simon, and L. Spiccia, Nanotechnology **18**, 125608 (2007).

[4] A. Wootsch, C. Descorme, S. Rousselet, D. Duprez, and C. Ternplier, Appl. Surf. Sci. **253**, 1310 (2006); C. P. Nicholas and T. J. Marks, Langmuir **20**, 9456 (2004).

[5] K. Kukli, M. Ritala, J. Aarik, T. Uustare, and M. Leskelä, J. Appl. Phys. **92**, 1833 (2002); M. Putkonen, J. Niinistö, K. Kukli, T. Sajavaara, M. Karppinen, H. Yamauchi, and L. Niinistö, Chem. Vap. Deposition **9**, 207 (2003); K. Kukli, J. Niinistö, A. Tamm, J. Lu, M. Ritala, M. Leskelä, M. Putkonen, L. Niinistö, F. Song, P. Williams, and P. N. Heys, Microelectron. Eng. **84**, 2010 (2007).

[6] S. Rushworth, K. Coward, H. Davies, P. Heys, T. Leese, L. Kempster, R. Odedra, and P. Williams, Surf. Coat. Technol. **201**, 9060 (2007).

[7] J. Niinistö, M. Putkonen, L. Niinistö, F. Q. Song, P. Williams, P. N. Heys, and R. Odedra, Chem. Mater. **19**, 3319 (2007).

[8] R. L. Puurunen, Chem. Vap. Deposition **9**, 249 (2003).

[9] Although reaction rates are governed by activation energies rather than bond enthalpies, the relative activation energies are likely to follow the same trends as bond enthalpies in this set of similar reactions.

[10] S. D. Elliott, Surf. Coat. Technol. **201**, 9076 (2007).

[11] R. Ahlrichs, M. Bär, M. Häser, H. Horn, and C. Kölmel, Chem. Phys. Lett. **162**, 165 (1989).

[12] A. D. Becke, Phys. Rev. A **38**, 3098 (1988); J. P. Perdew, Phys. Rev. B **33**, 8822 (1986).

[13] D. Andrae, U. Haussermann, M. Dolg, H. Stoll, and H. Preuss, Theor. Chim. Acta **77**, 123 (1990).

[14] A. Zydor, S. D. Elliott, T. Leese, F. Song, and S. Rushworth, ECS Trans. **11**, 113 (2007).

[15] J. Niinistö, A. Rahtu, M. Putkonen, M. Ritala, M. Leskelä, and L. Niinistö, Langmuir **21**, 7321 (2005); A. Rahtu and M. Ritala, J. Mater. Chem. **12**, 1484 (2002).

[16] J. W. Elam, M. D. Groner, and S. M. George, Rev. Sci. Instrum. **73**, 2981 (2002).

[17] *Eight Peak Index of Mass Spectra* (Mass Spectometry Data Centre, The Royal Society of Chemistry, Cambridge, UK, 1991), Vol. 1, p. 1.

[18] A. Schäfer, H. Horn, and R. Ahlrichs, J. Chem. Phys. **97**, 2571 (1992); K. Eichkorn, F. Weigend, O. Treutler, and R. Ahlrichs, Theor. Chem. Acc. **97**, 119 (1997).